

## THE HYDRODYNAMICS OF PHOTOIONIZED FLOWS

G. J. Ferland,<sup>1</sup> W. J. Henney,<sup>2</sup> R. J. R. Williams,<sup>3</sup> and S. J. Arthur<sup>2</sup>

### RESUMEN

Estamos trabajando para unir los elementos que son necesarios para hacer una descripción completa de la física y la hidrodinámica de plasmas, que permitan un modelaje autoconsistente de las regiones con líneas de emisión, como las regiones H II Galácticas (como Orión), las regiones H II extragalácticas y las galaxias con brotes de formación estelar luminosos. Estamos incorporando la hidrodinámica en Cloudy, un código de emisión de plasma que incluye la física necesaria para simular ambientes con gases ionizados, atómicos y moleculares. El flujo hidrodinámico desde la nube molecular hacia la región H II, pasando por la PDR, añade términos advectivos a los balances térmicos y de ionización, permitiendo que las regiones H II y PDR sean tratadas de forma autoconsistente. Esto permitirá explotar la región espectral del cercano al lejano IR y entender la evolución química en las sistemas huéspedes, así como la formación estelar a varias escalas. Nuestra primera aplicación se hace con Orión, el mejor estudiado de estos sistemas.

### ABSTRACT

We are working to bring together the ingredients necessary for a complete description of both the microphysics and the hydrodynamics of plasmas, allowing a self-consistent treatment of emission line regions such as those found in Galactic H II regions like Orion, extragalactic H II regions and luminous starburst galaxies. We are incorporating the necessary hydrodynamics into Cloudy, a plasma emission code that includes the physics needed to simulate the ionized, atomic, and molecular phases of the environment. The hydrodynamical flow, from the molecular cloud through the PDR into the H II region, brings advection terms into the thermal and ionization balance allowing both the H II region and PDR to be treated self-consistently. This will enable us to fully exploit the mid to far IR spectrum to understand the chemical evolution of the host system as well as star formation on many scales. Our first applications are to Orion, the best observed of these systems.

*Key Words:* **GALAXIES: STARBURST — H II REGIONS — HYDRODYNAMICS — STARS: FORMATION**

### 1. INTRODUCTION—THE H II REGION-PDR CONNECTION

The starburst phenomenon produces the most luminous objects in the universe, which can be used as probes of star formation and chemical evolution in the high redshift universe (Sanders & Mirabel 1996). The goals of present and future major IR missions, such as SOFIA, *SIRTF*, and *NGST*, are to understand fundamental galactic properties such as the chemical evolution of the interstellar medium (ISM) and the formation of clusters of stars with an associated initial mass function (IMF), and perhaps calibrate the sources as standard candles (Rowan-Robinson 2001; Thompson et al. 2001; Mao et al. 2000). At the same time, nearby H II regions such as Orion are a chance to study what is basically the same phenomenon, but at a much lower level of activity, and one where we have superb spatial and kinematic resolution.

Both starburst galaxies and Orion are likely to have the same underlying physics—a molecular cloud is exposed to ionizing radiation from a young star cluster. Heated material flows away from the molecular cloud becoming first atomic (the PDR) and eventually fully ionized (the H II region). In nearby H II regions it is possible to spatially resolve the gas as it accelerates. Both the PDR and the H II region are sources of strong emission lines, with species ranging from H<sub>2</sub>, CO, [C I], [O I], [C II], through higher ionization species such as H I, He I, [O III], and [Ne III]. Embedded grains produce the strong thermal infrared continuum. When properly interpreted, these lines and continua can be used to determine the form of the IMF, star formation rates, and chemical composition of the host ISM.

The material producing the observed emission is far from thermodynamic equilibrium. The concept of a temperature has little meaning, and the physical state of the gas is set by a host of microphysical processes. The incident and emitted radiation must be transferred through opaque media. The density of

<sup>1</sup>University of Kentucky, USA

<sup>2</sup>Instituto de Astronomía, UNAM, Morelia, México

<sup>3</sup>University of Wales, Cardiff, UK

the gas is set by the hydrodynamics of the flow from the molecular cloud through the H II region. This set of strongly intercoupled problems must be solved simultaneously to fully understand the information present in the observed spectrum.

Until now the PDR and H II region have been treated as two distinct problems. They are not: both the transport of gas and of radiation intimately link the two. Our goal is to develop the theoretical tools needed to understand the emission line regions on a holistic basis, and develop interpretive tools that have not been possible to date.

To this end, we are working to directly incorporate hydrodynamics into a complete plasma code Cloudy (Ferland et al. 1998; Ferland 2000). The code and its documentation are openly available on the web.<sup>4</sup> This development will make it possible to include dynamics in a typical spectral calculation, thus improving our ability to unravel the message hidden in the spectrum.

## 2. CURRENT STATUS OF H II REGION SIMULATIONS

The final state of the gas, and its observed spectrum, is the result of a host of microphysical processes. In the H II region, the dominant heating processes are photoionization of hydrogen and grains (for example, Baldwin et al. 1991), and the dominant cooling is by collisional excitation of the observed optical and IR forbidden lines (Osterbrock 1989). In the PDR, the dominant heating processes are photoionization of grains, line absorption of the IR continuum, and cooling by collisional excitation of IR forbidden lines (Hollenbach & Tielens 1999). Both regions emit IR lines and continua; indeed many lines ([C II]  $\lambda$  158  $\mu$ m, [O I]  $\lambda$  63  $\mu$ m) are formed in both regions.

The current version of Cloudy includes all atomic fine-structure transitions for lines from all stages of ionization of the first thirty elements (H–Zn) with known atomic data (mostly the result of the Iron Project, see Hummer et al. 1993). These include the infrared lines mostly commonly produced and observed from a photoionized gas. Atoms of the hydrogenic isoelectronic sequence and the helium isoelectronic sequence are modeled as large multilevel atoms (typically 50 levels per ion, but coded so that the number of levels is limited only the processor power). All lines are transferred including continuum pumping, destruction by background opacity sources, and thermalization.

The molecule network presently includes  $\text{H}^-$ ,  $\text{H}_2$ ,

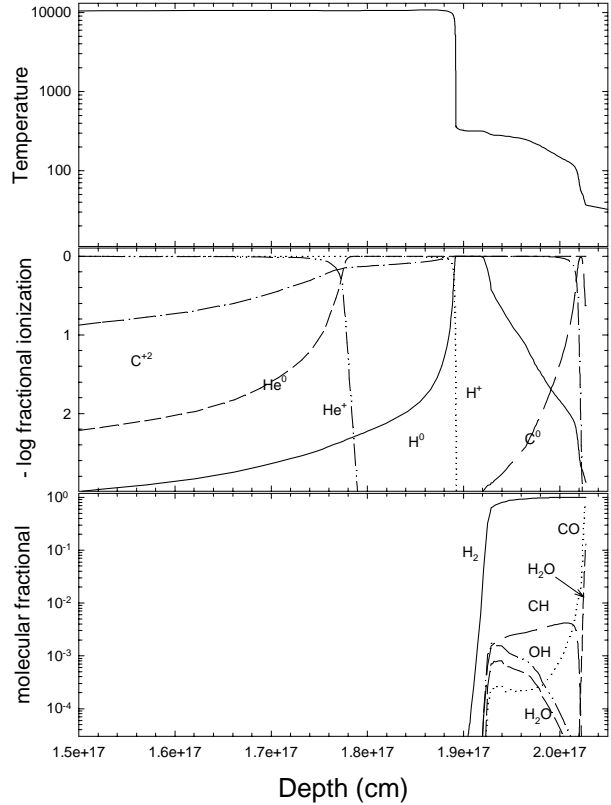


Fig. 1. The computed thermal (top), atomic ionization (middle), and molecular (bottom) structure of a constant gas pressure H II region and PDR similar to Orion. The depth from the illuminated face of the layer is the independent axis. The interface between the H II region and PDR occurs at a depth of  $\approx 1.9 \times 10^{17}$  cm. The gas density within the PDR is several orders of magnitude greater than the density in the H II region, due to the constant gas pressure assumption, so far more mass is located in the PDR than in the H II region.

$\text{H}_2^+$ ,  $\text{H}_3^+$ ,  $\text{HeH}^+$ , OH,  $\text{OH}^+$ , CH,  $\text{CH}^+$ ,  $\text{O}_2$ ,  $\text{O}_2^+$ , CO,  $\text{CO}^+$ ,  $\text{H}_2\text{O}$ ,  $\text{H}_2\text{O}^+$ ,  $\text{H}_3\text{O}^+$ , and  $\text{CH}_2^+$ . Reaction rate coefficients are from Hollenbach & McKee (1979; 1989); Tielens and Hollenbach (1985), Lenzuni, Chernoff, & Salpeter (1991), and Wolfire, Tielens, & Hollenbach (1990); Crosas & Weisheit (1993); Puy et al. (1993), and “The UMIST Database”<sup>5</sup> The resulting chemistry is in good agreement with standard PDR calculations.

CO includes both  $^{12}\text{C}^{16}\text{O}$  and  $^{13}\text{C}^{16}\text{O}$  using shielding rates from van Dishoeck & Black (1988) and all radiative transfer processes. These molecules are treated as rigid rotators, with a complete calculation of the level populations and emission from the ground rotational ladder. Any number of levels can be included and collision rates from de Jong, Chu,

<sup>4</sup>See <http://nimbus.pa.uky.edu/cloudy>.

<sup>5</sup><http://www.rate99.co.uk/>

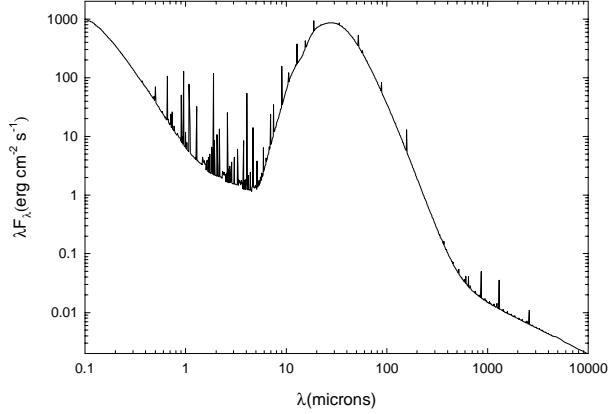


Fig. 2. The full spectrum from the Orion H II region and PDR.

& Dalgarno (1975) are used. The effects of supra-thermal electrons are important in the PDR, even in Orion (due to the transmitted diffuse X-ray continuum discussed below) and knock-on secondary ionization rates are treated as in Dalgarno et al. (1999).

A major effort has gone into making the grain physics state-of-the-art. The current implementation is described by van Hoof, Weingartner, et al. (2001). A built-in Mie code can be used to generate optical properties for any grain constituent, and the grain population can be resolved into any number of size bins. Grain charging, heating, temperature and drift velocity are then computed for each size (e.g., Baldwin et al. 1991). Resolving the grain size distribution is crucial since smaller grains tend to be hotter, produce the greatest photoelectric heating of the gas, and so have a profound effect on the spectrum. PAHs and single-photon heating (Guhathakurta & Draine 1989) are also fully treated. The current implementation of the grain physics fully reproduces the results presented by Weingartner et al. (2001) but with the added advantage of including a self-consistent solution of the physical state of the gas surrounding the grains (radiation field, electron kinetic energy distribution, etc).

Figure 1 shows the ionization and thermal structure predicted by a calculation of an isobaric H II region and PDR. Parameters are chosen to be similar to those in inner regions of Orion, close to the Trapezium stars (Baldwin et al. 1991). Although we assume constant gas pressure to join the H II region and PDR for this illustration, our goal is to self-consistently connect these by solving the underlying hydrodynamics.

Figure 2 shows the full spectrum emitted by this geometry. There is a strong thermal infrared continuum from the photo-heated grains, and strong ionic,

atomic, and molecular emission lines. These continua and lines are all diagnostic indicators of the properties of the emitting gas, and can be used to deduce the gas composition, dust to gas ratio, and the form of the ionizing continuum (and hence investigate the properties of the central stars).

In the past the H II region and PDR have been treated as totally separate problems, using spectral UV/optical/IR signatures to derive independent parameters for each. In an ideal world, they would be treated together, with the H II region a simple continuation of the PDR and the properties of both determined by hydrodynamical flow equations.

### 3. HYDRODYNAMICS IN A PHOTOIONIZED ENVIRONMENT

In the simplest case, the instantaneous turn-on of a star in a uniform density cloud, the evolution of an expanding H II region goes through several distinct stages. At first the expansion is rapid with many ionizing photons arriving at the ionization front. This R-type ionization front has nearly the same density on either side, but a large jump in temperature across the front. The flux of photons striking the front decreases as the front moves out, and the ionization front evolves from R-type to D-type, eventually (if the star lives long enough) tending towards the extreme weak-D front that is approximated by the constant-pressure cloud considered above.

However, it is known that real-world H II regions rarely follow such a tidy pattern—a result of the chaotic and clumpy nature of the environment in which massive stars are born. In fact, observational selection effects lead to the brightest and most spectacular H II regions (variously described as champagne flows, H II blisters, or photoevaporation flows) generally having strong-D or D- critical ionization fronts, which slowly eat into dense molecular cores and clumps (e.g., Bertoldi & Draine 1996; Henney 2001). The Orion nebula is a prime example of this type of region and the vast quantity of high quality observations of this object, including spatially-resolved, high-resolution spectroscopy in many atomic and ionic species (Balick et al. 1974; Baldwin et al. 2000). Orion offers a unique opportunity for critically testing photoionization models which can then be applied to more luminous regions in starburst galaxies where the observations are necessarily less rich.

The calculations presented here center on the weak-D phase. We hope to progress to the R and strong-D fronts that are likely to be found earlier in the evolution of a star cluster. Solutions involving the strong-D and D-critical fronts have wide ap-

plication since these are also likely to describe the photoevaporation of gas from a cometary globule (O'Dell, Henney, & Burkert 2000), proplyd (Henney & Arthur 1998; Henney et al. 2001) or photoionized column (Williams, Ward-Thompson, & Whitworth 2001).

### 3.1. Structure and advection

Several levels of approximation can be introduced in the solution to the general hydrodynamics problem. For any species A, possibly an ionic or molecular density, the full conservation equation will take a general form

$$\begin{aligned} \frac{D}{Dt}(A/\rho) &\equiv \frac{\partial}{\partial t}(A/\rho) + \mathbf{u} \cdot \nabla(A/\rho) \\ &= (\text{sources} - \text{sinks}). \end{aligned} \quad (1)$$

Here the first term on the right hand side represents changes in the system over time, and the second term is the advection of fresh material from upstream (away from the star cluster). This is equal to the rate new material enters, perhaps as the result of new mass introduced by loss from embedded objects. In a steady-state flow the first term is zero. The second term may be small if conditions do not change across the region.

For a steady-state flow, the standard equations of motion for a compressible fluid, in a plane-parallel geometry appropriate for a blister on a molecular cloud, may be written as

$$\frac{\partial}{\partial x}(\rho u) = 0, \quad (2)$$

$$\frac{\partial}{\partial x}(p + \rho u^2) = \rho a, \quad (3)$$

$$\frac{\partial}{\partial x} \left[ \rho u \left( w + \frac{1}{2} u^2 \right) \right] = \rho Q, \quad (4)$$

$$\frac{\partial}{\partial x}(n_i u) = n_i \sum_j R_{ij} - \sum_j n_j R_{ij}. \quad (5)$$

Here  $a$  is the acceleration e.g., gravity or radiation pressure,  $w$  is the specific enthalpy  $w = \varepsilon + p/\rho$  where  $\varepsilon$  is the specific internal heat, and  $Q$  is heating minus cooling. With a full solution these lead to a description of the cloud density as a function of depth (needed to fully integrate the H II region and PDR problems) and also include terms that enter the ionization and thermal balance of the gas and grains in both regions.

Most plasma codes implicitly ignore the terms on the left hand sides of these equations, solving for

ionization and thermal equilibrium for a predetermined density distribution, and no ordered velocity field. Under this assumption, equation (1) can be rewritten as sources = sinks. This leads to the usual forms of the statistical and thermal balance equations given in standard references, for instance, Aller (1984); Osterbrock (1989); Davidson & Netzer (1979); and Netzer (1990).

We are now focusing on the broad class of astronomical objects where the flow is close to being in a steady state. Then the rate at which atoms leave any level  $j$  is modified by advection and given by

$$\frac{\partial n_j}{\partial t} = -\frac{\partial}{\partial x}(u n_j) + n_j \sum_{k \neq j} (n_k R_{kj} - n_j R_{jk}), \quad (6)$$

and the corresponding energy equation will be similar to

$$\begin{aligned} \frac{\partial U}{\partial t} &\equiv \frac{\partial}{\partial t} \left( \frac{3}{2} \sum_j n_j kT \right) \\ &= G - L + \frac{p}{\rho} \frac{\partial \rho}{\partial t} - U \nabla \cdot \mathbf{u}, \end{aligned} \quad (7)$$

where  $U$  is the internal energy and where  $G$  and  $L$  and the energy gains and losses per unit time, and  $u$  the velocity.

Ignoring the dynamical terms is a good assumption when the physical conditions across a flow change more slowly than the atomic timescales. This is likely to be the case within the H<sup>+</sup> region of H II regions, but is not likely to be the case close to any ionization front (e.g., the H<sup>+</sup>-H<sup>0</sup> or He<sup>+</sup>-He<sup>0</sup> fronts).

Progress in incorporating hydrodynamics into plasma codes has been slow. Harrington (1977) studied the case of a weak-D front and found that optical and UV emission lines changed by only 10 to 30%. This has been used as justification for not including this physics in plasma codes. (The effects of advection should be much larger in the strong-D or D-critical cases that apply to the photoevaporation regions we will consider.) The class of "shock codes" (Daltabuit & Cox 1972; Raymond 1979; Dopita & Sutherland 1996) also include much of the appropriate physics, but have not been applied to the predominantly photoionized star-forming regions we consider, nor to dusty molecular regions.

## 4. WHY THIS IS HARD

The fact that plasma and hydrodynamical numerical approaches have not been fully integrated is the result of the historical gap between the two communities, a gap that we are trying to bridge, but

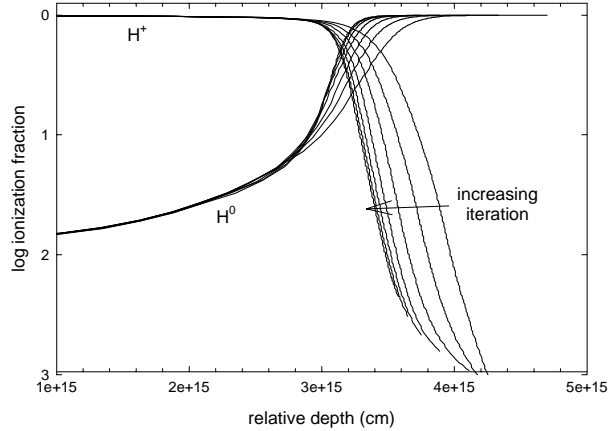


Fig. 3. The  $H^0$ - $H^+$  ionization front on successive iterations, with advection included. The advected material, flowing from the right, pushes the ionization front to the left.

also reflects the fact that computers were simply not powerful enough to do the full problem in the past. The existence of fast cheap processors makes this the time to solve the full problem.

Within the plasma code community the most common approach to simulating the dynamics of a flow such as an H II region or quasar cloud is to make a static simplification to the dynamical solution. Isochoric (constant density), isobaric (constant pressure), or hydrostatic solutions are common. Another approach is to treat the hydrodynamics as an external problem and compute the geometry and resulting flow independently of the plasma microphysics. The resulting solution is then fed into a photoionization code as a prescribed density law, and the resulting ionization structure and spectrum is then computed. This may be better than doing nothing, but it is not self-consistent, and the solution will likely violate many conservation laws.

The fundamental difficulty in coupling a true radiative transfer/microphysics simulation with a hydrodynamics calculation is that the two problems do not share common boundary conditions. A photoionized cloud has a well-established boundary condition at the illuminated face of the cloud—the incident radiation field is known here, and the gas density is set as a free parameter. The radiation field is transported into the cloud and attenuated with depth. The radiation field at a particular point will depend mostly on the cumulative effects of the absorption and emission from gas between the illuminated face and the point in question (although emission from gas further away from the ionizing source must be included). So the photoionization solution

must begin at the illuminated face of the cloud. This contrasts with the hydrodynamical flow, which begins where the gas is cold and neutral. Many methods of solution proceed downstream to the illuminated face. The essence of the difference is that in photoionization, you follow the photons (which mostly go away from the star), while in hydrodynamics you must follow the particles (which mostly go towards it), and the sound waves.

The sonic point is a second problem, being where one of the sound waves changes direction in the steady flow frame (Williams & Dyson 1996; Williams 2001). For steady state flows, integrals of motion constrain the hydrodynamic solution. These integral constraints have multiple solutions: in very sub-sonic and very-supersonic flows, the relevant solution is generally obvious, and much previous work has centered on one of these limits. At intermediate flow speeds, care has to be taken to find solutions which smoothly pass through the critical speed.

## 5. THE PROJECT

Plasma codes search for equilibrium solutions of the ionization equations. While it would be possible to re-code the ionization equations in an explicitly time-dependent fashion, this structure in fact works to our advantage. The photoionization terms in the steady-state solution will often have very short timescales. If we attempt to integrate these stiff equations explicitly, stability constraints will limit our time step to the short photoionization time (Harrington 1977 discusses this problem). Instead we have developed a new approach, which takes advantage of the current algorithm. To see this we first rewrite equation (4) as

$$\frac{\partial W}{\partial x} = Q. \quad (8)$$

The solution is to difference the equations implicitly, i.e. to solve

$$W_{i+1} = Q_i(W_i)\Delta x + W_i \quad (9)$$

for  $W_i$ . This form is exactly that required for the equilibrium search to find the solution. A similar differencing scheme can be applied to the other dynamical equations, although care has to be taken to select the correct solution of the momentum equation, 3.

We have implemented the initial parts of this into Cloudy. Figure 3 shows part of the computed structure near the  $H^0$ - $H^+$  ionization front. This is the simplest case of a constant-velocity, time-steady flow. The flow is from right to left at a constant

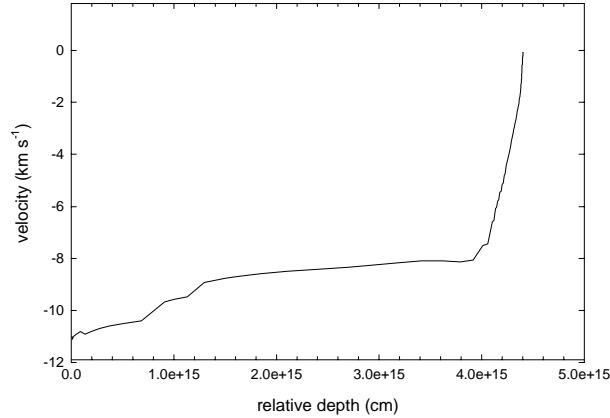


Fig. 4. The computed velocity structure of an H II region somewhat similar to, but not exactly the same as those given above. The velocity is determined self-consistently, but neglecting advection.

speed typical of D-critical ionization fronts. The position of the ionization front moves to the left as advected neutral material is added to the ionized gas. Convergence is obviously fairly rapid.

We have also made preliminary advances in the methods needed to self-consistently solve for the velocity as a function of depth. Figure 4 shows a computed velocity structure for a calculation somewhat similar to those presented above, but without the advection terms. The acceleration of the gas as it moves through the ionization front is dramatic, and the gas coasts through the H II region itself, in general agreement with the observed velocity profiles in Orion (Balick et al. 1974; Baldwin et al. 2000).

The dynamics have significant effects on the observed spectrum. Table 1 gives intensities of some of the lines emitted by the H II region and PDR for the case illustrated in Figure 3. Spectra for both the static and dynamic situations are listed.

## 6. LINE PROFILES

Since the gas velocity and all other physical conditions are known at each point in the simulations, it is a straightforward matter to calculate the predicted line profile in a given emission line. Examples of predicted mean velocities and FWHM are shown in Figure 5 for a range of models, whose parameters were chosen to be close to the conditions of the principal ionization front in the central regions of the Orion nebula. The models differ in the details of the incident ionizing spectrum, the gas velocity at the illuminated face and whether or not continuum radiation pressure is included. All are plane-parallel and represent weak D fronts, in which the flow is everywhere subsonic (maximum Mach number reached

TABLE 1  
ADVECTION AND THE RESULTING SPECTRUM

Line	Static	Advection
H $\beta$	100.	100.
$L(\text{Grain IR})$	14.3	9.56
CO $\lambda$ 862 $\mu\text{m}$	0.0063	0.013
C II] $\lambda$ 2325 $\text{\AA}$	62.0	62.1
[C II] $\lambda$ 157 $\mu\text{m}$	0.47	0.37
[O III] $\lambda$ 5007 $\text{\AA}$	4.9	5.6
[O II] $\lambda$ 3727 $\text{\AA}$	236.	238.
[O I] $\lambda$ 6300 $\text{\AA}$	9.09	4.54
[O I] $\lambda$ 63 $\mu\text{m}$	2.18	0.93
[Ne II] $\lambda$ 12.8 $\mu\text{m}$	37.8	36.9
[Si II] $\lambda$ 34.8 $\mu\text{m}$	1.91	1.62

= 0.4–0.6). Also shown for comparison are the mean observed blueshifts with respect to the molecular gas ( $V_{\odot} \simeq 28 \text{ km s}^{-1}$ ) of lines from the central region of the Orion nebula (Henney & O’Dell 1999).

It is noteworthy that the models all fail to reproduce the observed strong acceleration with increasing ionization potential that was first noted by Kaler (1967). All the models show a very slight acceleration ( $\simeq 1 \text{ km s}^{-1}$ ) between [O I] and [S II]/[N II] but this is much less than the observed velocity difference. Furthermore, only the D10 model shows any significant acceleration between [N II] and [O III] and this is again rather less than that observed, although it is possible that strong-D models including geometrical divergence may overcome this last discrepancy.

The model linewidths (Fig. 5, lower panel) are also all much less than those that are observed in Orion, where the non-thermal contribution to the FWHM is typically  $\simeq 10 \text{ km s}^{-1}$ . In this case too, geometrical divergence may help increase the predicted linewidths.

GJF thanks the NSF and NASA for support through grants AST-0071180 and NAG5-8212. SJA and WJH acknowledge support from project IN117799 DGAPA-PAPIIT, UNAM, México.

## REFERENCES

- Aller, L. H. 1984, *Physics of Thermal Gaseous Nebulae* (Dordrecht: Reidel)
- Baldwin, J., Ferland, G. J., Martin, P. G., Corbin, M., Cota, S., Peterson, B. M., & Slettebak, A. 1991, *ApJ*, 374, 580
- Baldwin, J. A., Verner, E. M., Verner, D. A., Ferland, G. J., Martin, P. G., Korista, K. T., & Rubin, R. H. 2000, *ApJS*, 129, 229

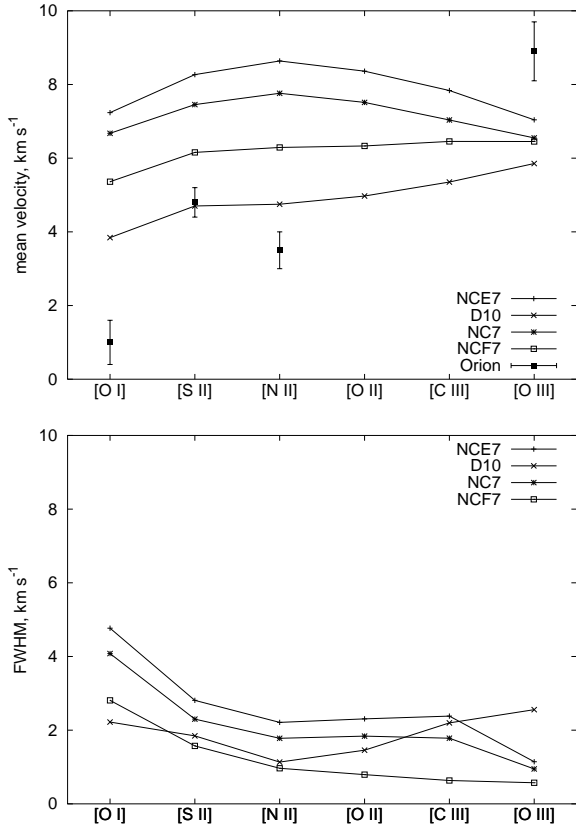


Fig. 5. Line profile characteristics of optical/NUV emission lines from different plane-parallel weak-D Cloudy models, assuming a face-on viewing orientation, compared with typical observed values for the Orion nebula.

Balick, B., Gammon, R. H., & Hjellming, R. 1974, *PASP*, 86, 616  
 Bertoldi, F., & Draine, B. T. 1996, *ApJ*, 458, 222  
 Crosas, M., & Weisheit, J. C. 1993, *MNRAS*, 262, 359  
 Dalgarno, A., Yan, M., & Liu, W. 1999, *ApJS*, 125, 237  
 Daltabuit, E., & Cox, D., 1972, *ApJ*, 173, L13  
 Davidson, K., & Netzer, H. 1979, *Rep. Prog. in Physics*, 51, 715  
 de Jong, T., Chu, S.-I., & Dalgarno, A. 1975, *ApJ*, 199, 69  
 Dopita, M., & Sutherland, R. S., 1996, *ApJS*, 102, 161  
 Ferland, G. J., 2000, *RevMexAA(SC)*, 9, 153  
 Ferland, G. J., Korista, K. T., Verner, D. A., & Dalgarno, A. 1997, *ApJ*, 481, L115  
 Ferland, G. J., Korista, K. T., Verner, D. A., Ferguson, J. W., Kingdon, J. B., & Verner, E. M. 1998, *PASP*,

110, 761  
 Guhathakurta, P., & Draine, B. T. 1989, *ApJ*, 345, 230  
 Harrington, J. P. 1977, *MNRAS*, 179, 63  
 Henney, W. J. 2001, *RevMexAA (SC)*, 10, 57  
 Henney, W. J., & Arthur, S. J. 1998, *AJ*, 116, 322  
 Henney, W. J., & O'Dell, C. R. 1999, *AJ*, 118, 2350  
 Henney, W. J., O'Dell, C. R., Meaburn, J., Garrington, S. T., López, J. A. 2001, *ApJ* in press  
 Hollenbach, D., & McKee, C. F. 1979, *ApJS*, 41, 555  
 Hollenbach, D., & McKee, C. F. 1989, *ApJ*, 342, 306  
 Hollenbach, D. J., & Tielens, A. G. G. M. 1999, *Rev. Mod. Phys.*, 71, 173  
 Hummer, D. G., Berrington, K. A., Eissner, W., Pradhan, A. K., Saraph H. E., Tully, J. A. 1993, *A&A*, 279, 298  
 Kaler, J. B. 1967, *ApJ*, 148, 925  
 Lenzuni, P., Chernoff, D. F., & Salpeter, E. E. 1991, *ApJS*, 76, 759  
 Mao, R. Q., Henkel, C., Schulz, A., Zielinsky, M., Mauersberger, R., Störzer, H., Wilson, T. L., & Gensheimer, P. 2000, *A&A*, 358, 433  
 Netzer, H. 1990, in *Saas-Fee Advanced Course, Vol. 20, Active Galactic Nuclei*, eds. T. J.-L. Courvoisier & M. Mayor, (Berlin: Springer-Verlag), 57  
 O'Dell, C. R., Henney, W. J., & Burkert, A. 2000, *AJ*, 119, 2910  
 Osterbrock, D. E. 1989, *Astrophysics of Gaseous Nebulae & Active Galactic Nuclei* (Mill Valley: University Science Press)  
 Puy, D., Alecian, G., Le Bourlot, J., Leorat, J., & Pineau des Forets, G. 1993, *A&A*, 267, 337  
 Raymond, J. C. 1979, *ApJS*, 39, 1  
 Rowan-Robinson, M. 2001, *ApJ*, 549, 745  
 Sanders, D. B., & Mirabel, I. F. 1996, *ARA&A*, 34, 749  
 Schulz N. S., Canizares, C., Huenemoerder, D., Kastner, J. H., Taylor, S. C., & Bergstrom, E. J. 2001, *ApJ*, 549, 441  
 Thompson, R. I., Weymann, R. J., & Storrie-Lombardi, L. J. 2001, *ApJ*, 546, 694  
 Tielens, A. G. G. M., & Hollenbach, D. 1985, *ApJ*, 291, 722  
 van Dishoeck, E. F., & Black, J. H. 1988, *ApJ*, 334, 771  
 Weingartner, J. C., & Draine, B. T. 2001, *ApJS*, 134, 263  
 Williams, R. J. R. 2000, *MNRAS*, 316, 803  
 Williams, R. J. R. 2001, *MNRAS*, 325, 293  
 Williams, R. J. R., & Dyson, J. E. 1996, *MNRAS*, 279, 987  
 Williams, R. J. R., Ward-Thompson, D., & Whitworth, A. P. 2001, *MNRAS*, 327, 788  
 Wolfire, M. G., Tielens, A., & Hollenbach, D. 1990, *ApJ*, 358, 116

Gary J. Ferland: Department of Physics & Astronomy, University of Kentucky, 177 Chem.-Phys. Building, 600 Rose Street Lexington, Kentucky 40506-0055, USA (gary@pop.uky.edu).  
 William J. Henney and S. Jane Arthur: Instituto de Astronomía, UNAM Campus Morelia, Apdo. Postal 3-72 (Xangari), 58089 Morelia, Michoacán, México (w.henney,j.arthur@astro.unam.mx).  
 Robin J. R. Williams: Department of Physics and Astronomy, Cardiff University, PO Box 913, Cardiff, CF24 3YB, UK (Robin.Williams@astro.cf.ac.uk).